Canadian Conference - Pacific Conference on Earthquake Engineering 2023
Vancouver, British Columbia
June 25th – June 30th, 2023

A Proposed Seismic Site Response Analysis Approach Consistent with the 6th Generation Seismic Hazard Model of Canada

Chris Weech[1], Armin Bebamzadeh[2], Mike Fairhurst[2], Roberto Olivera[3], Carlos Ventura[4]

[1]Senior Geotechnical Engineer, Thurber Engineering, Victoria, BC, Canada
[2]Researcher, Earthquake Engineering Research Facility, University of British Columbia, Vancouver, BC, Canada
[3]Associate, WSP Canada, Vancouver, BC, Canada
[4]Professor, Department of Civil Engineering, University of British Columbia, Vancouver, BC, Canada

ABSTRACT

In the 6th Generation Seismic Hazard Model of Canada (SHMC-6), multiple ground motion models (GMMs) are used to calculate hazard values at ground surface which include site amplification effects calculated internally using V_{s30}-dependent site terms specific to each GMM. Non-linear amplification effects are calculated as a function of the median prediction of ground motion intensity associated with each event scenario considered in the hazard model. Exceedance rates of the amplified ground motion values for each event scenario are then aggregated to generate the suite of probabilistic hazard curves.

A method of conducting seismic site response analysis (SSRA) using acceleration time histories that have been scaled to the median peak ground acceleration for the reference ground condition (*med_PGA$_{ref}$*), referred to as the Median Intensity Target (MIT) approach, is proposed. For time history selection, target response spectra comprising median hazard values can be determined from the Uniform Hazard Spectrum (UHS) using the GMM sigma values and the mean epsilon obtained from deaggregation of the UHS values for the reference ground condition. Mean amplification functions conditioned on the *med_PGA$_{ref}$* that is specific to each tectonic regime type (TRT), $\bar{F}(T, med\_PGA_{ref})_{TRT}$, are determined from SSRA conducted on each suite of time histories. The site-specific UHS is obtained by multiplying the UHS for the reference ground condition by the contribution-weighted mean $\bar{F}(T)$ for the total hazard, $\bar{F}(T)_{TH}$.

Implementation of the proposed MIT approach is described using an example of a short-period site having a strong impedance contrast due to clay overlying shallow bedrock, located in Victoria, BC. The $\bar{F}(T)_{TH}$ determined for this example site is shown to be in excellent agreement with the average amplification function determined from the Rigorous Method which involved calculating the site-specific UHS directly from SHMC-6 after modifying the OpenQuake code to replace the GMM site terms with tables of SSRA-derived $F(T,PGA_{ref})$ calculated for a range of PGA_{ref} that varied from 0.05g to 0.60g.

Keywords: seismic site response analysis, amplification function, median ground motion intensity

INTRODUCTION

The 6th Generation Seismic Hazard Model of Canada (SHMC-6) has been adopted for the 2020 National Building Code of Canada (NBC 2020). For any geographic location in Canada, the SHMC calculates a suite of probabilistic seismic hazard values comprising 5% damped response spectrum accelerations, $S_a(T)$, at various periods of vibration, T, along with values of peak ground acceleration (PGA) and peak ground velocity (PGV). In SHMC-6, the seismic hazard values are generated using a logic tree approach with multiple ground motion models (GMMs), as described by Kolaj et al., 2019 [1].

Seismic Hazard Model of Canada

The modelling of seismic hazard In Southwestern British Columbia involves consideration of the contributions from three different tectonic regime types (TRTs):

- crustal earthquakes within the tectonically active North American Cordillera (crustal events),
- megathrust events (M_w > 8) along the Cascadia subduction interface (interface events), and
- earthquakes originating from within the subducting Juan de Fuca plate (in-slab events).

In SHMC-6, each of these TRTs is modelled using a suite of 4 different GMMs, each having a 25% probability weighting in the logic tree. Each GMM includes a period-dependent "sigma" model, $\sigma(T)$, to account for aleatoric uncertainty associated with between-event and within-event variability [1]. Sigma is the standard deviation (in natural logarithm units) that is associated with the statistical fit of the GMM-predicted hazard value to the earthquake database from which the GMM was derived.

In both SHMC-6 and the previous SHMC-5, hazard values for each event scenario within the hazard model are estimated using the relevant GMM(s). The event-specific hazard value estimate and the sigma from each GMM are combined with the probability of occurrence of the event scenario (obtained from magnitude-recurrence relationships) to determine the annual exceedance rates (AER) corresponding to a wide range of trial hazard values. For each trial hazard value, the individual AER_i associated with each event scenario considered by the hazard model are summed to calculate the total hazard AER (AER_T) for all event scenarios. The probabilistic hazard curve for each hazard value describes the variation of AER_T with trial hazard value intensity. The design hazard value corresponding to a specified AER_T (eg. 0.000404 per annum corresponding to a 2% probability of exceedance in 50 years) are then obtained from the hazard curve. The Uniform Hazard Spectrum (UHS) is the set of $S_a(T)$ at all the code-specified periods which all have the same AER_T.

In NBC 2015, site amplification was calculated using period-specific amplification factors for each site class, $F(T,PGA_{ref})$, which were a function of the aggregated probabilistic PGA corresponding to the Site Class C reference condition. For Site Classes D and E, $F(T,PGA_{ref})$ at all periods decreased as PGA_{ref} increased from 0.1g to 0.5g to account for increased damping that occurs at higher shear strains.

Each GMM in SHMC-6 calculates site amplification effects using linear and non-linear site amplification terms that are a function of the time-weighted average shear wave velocity (V_s) to a depth of 30 m below ground surface, V_{s30}. Non-linear amplification effects are calculated based on the median (50% probability of exceedance) prediction of ground motion intensity associated with each event scenario corresponding to a particular magnitude-distance (M-R) combination from a particular TRT. A short-period ground motion parameter (typically PGA) for a rock reference condition is typically used as the ground motion intensity measure (IM) for calculating the non-linear site term in most of the GMMs [1].

Code-Consistent Seismic Site Response Analysis

It has been standard practice to conduct a Seismic Site Response Analysis (SSRA) using earthquake acceleration time histories that are scaled and/or spectrally matched to a target response spectrum corresponding to the UHS at the design hazard level for the seismic site class that best represents the ground conditions within the elastic half space at the base of the soil column (herein referred to as the UHS Target approach). Thus, the site-specific seismic hazard values generated from each time history analysis are only applicable to the amplification response of the site to ground motion intensities corresponding to the aggregated seismic hazard at that location. This approach is consistent with the approach adopted by NBC 2015, in which the amplification factors for Site Classes D and E are a function of PGA_{ref} associated with the design-basis aggregated hazard.

However, SSRA conducted using ground motion intensities consistent with aggregated probabilistic hazard values will tend to produce estimates of shear strains that are much higher than what would be expected from analysis of the individual earthquake event scenarios considered by the seismic hazard model. The higher shear strains result in over-estimation of the degree of soil non-linearity, as characterized by increased shear modulus reduction and hysteretic damping, which tends to reduce soil amplification, particularly at short periods. The UHS Target Approach is not consistent with the SHMC-6 approach to estimating non-linear amplification effects based on the median prediction of ground motion intensity associated with individual event scenarios.

This paper describes a simplified method of conducting a SHMC-6-consistent SSRA using acceleration time histories that are scaled to the median PGA of the reference ground condition, med_PGA_{ref}, as determined from deaggregation of PGA_{ref} at the design hazard level. This paper will show that the single amplification function that is generated using this simplified approach (herein referred to as the Median Intensity Target approach) produces an amplified UHS that is very similar to the UHS that is generated using a modified version of SHMC-6 in which the GMM site terms are replaced by lookup tables of SSRA-derived amplification factors that vary as a function of ground motion intensity (herein referred to as the Rigorous Method). The Rigorous Method, which is discussed later in this paper, is described in a companion paper by Bebamzadeh et al., 2023 [2].

SEISMIC SITE RESPONSE ANALYSIS PILOT STUDY

A pilot study was carried out to test how SSRA results can be implemented within the SRG2020 Analyzer that was developed for structural analysis of seismic retrofits for low-rise buildings in British Columbia and has recently been adapted to be compatible with SHMC-6. As part of that study, 1D SSRA were carried out on an example soil profile from a site located at the Legislative Assembly of BC in downtown Victoria, BC. The computer program DEEPSOIL v7.0 was used to conduct linear, equivalent-linear and non-linear analyses.

SSRA Methodology

The ground conditions analyzed are typical for Victoria, comprising a 9.1 m thickness of low plasticity glaciomarine clay with a variable shear wave velocity profile overlying bedrock belonging to the Lower Paleozoic Wark Gneiss formation. The upper 5 m thickness of clay comprises a very stiff to hard crust that is highly overconsolidated due to desiccation, which is underlain by stiff to firm clay that is moderately to lightly overconsolidated. The variation in V_s, soil unit weight, plasticity index, and dynamic undrained shear strength, s_{u_EQ}, with depth (z) within the soil profile that was adopted for the SSRA, are plotted in Figure 1. The time-weighted average V_s of the soil, $(\overline{V}_s)_{soil}$, is 166 m/s. For this pilot study, a V_s in rock, V_{s_rock}, of 1100 m/s was assigned to the elastic half space at the base of the soil column (rather than attempting to model the true $V_s(z)$ gradient in the top of the bedrock at the site). This is a high-impedance site where strong resonant amplification of ground motion frequencies near the fundamental frequency of the site had been identified through previous studies. Using an equivalent single layer (ESL) model, the linear-elastic response of the soil column can be expected to have a fundamental period (first mode of vibration), $T_0 = 4H/(\overline{V}_s)_{soil}$ of 0.22s.

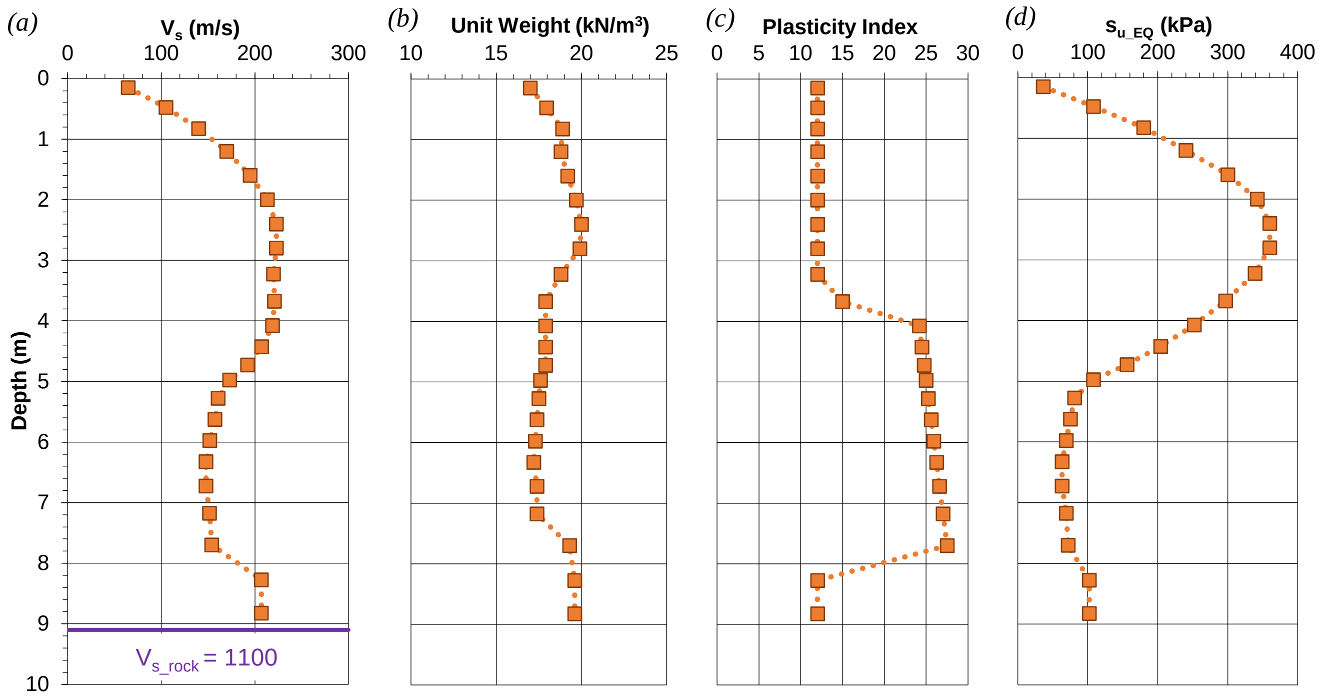

Figure 1. SSRA Input Parameter Profiles: (a) Shear Wave Velocity, (b) Unit Weight, (c) Plasticity Index, (d) Dynamic Undrained Shear Strength.

The SSRA was conducted using a suite of 11 horizontal acceleration time histories for each of the three TRTs (crustal, in-slab and interface). The outcropping motions to be input into the SSRA were selected by initially scaling the 5% damped horizontal acceleration response spectrum of each record so that the geomean of each suite was a reasonably close fit to the TRT-specific UHS at the 2% probability of exceedance in 50 years (2%/50-years) hazard level. Spectral matching to the target spectrum was not carried out at any periods thereby preserving the spectral variability in the original records and the variation in frequency content with time within each record.

In the linear analysis, the ground response was purely a function of the small-strain shear modulus, G_{max}, which is computed directly from V_s, and the small-strain damping ratio, D_{min}, neither of which vary with shear strain. Equivalent-linear (EL) SSRA accounts for changes in secant shear modulus (G) and damping ratio (D) with increasing shear strain (γ_{cyc}) using modulus reduction and damping curves (MRDC) derived from laboratory tests. The MRDC used in EL analyses can reasonably capture non-linear soil behaviour when γ_{cyc} is less than about 0.3% strain. The EL SSRA in this study were conducted in the frequency domain using the pressure-dependent shear modulus reduction (G/G_{max} vs γ_{cyc}) and damping (D vs γ_{cyc}) curves by Darendeli, 2001 [3].

A limitation of the EL method is that soil shear strength is not explicitly considered so the stress-strain behaviour of the soil does not tend to be properly represented as cyclic shear stresses approach the shear strength of the soil. In a non-linear (NL) analysis, the non-linear stress-strain curve is explicitly considered, with the shear stress becoming asymptotic with the user-defined shear strength at large strains. The General Quadratic/Hyperbolic (GQ/H) model in DEEPSOIL was used to model the non-linear stress-strain response in the NL analysis, which was conducted in the time domain. The GQ/H model parameters were assigned by fitting the NL MRDC to the EL MRDC.

For the Rigorous Method, a set of SSRA-based amplification functions, F(T), which correspond to the ratio of site-specific $S_a(T)$ at ground surface to the $S_a(T)_{ref}$ for the reference condition, were developed for various ground motion intensity levels that would be applicable to the range of intensities associated with individual event scenarios. In this study, V_{s30} = 1100 m/s was used as the reference condition and PGA was selected as the IM for determining F(T) as a function of PGA_{ref}, which is consistent with the approach used by most of the GMMs in SHMC-6. From SHMC-6, the total hazard PGA_{ref} at 2%/50-years is 0.58g at the example site location. Therefore, intensity levels corresponding to PGA_{ref} = 0.05g, 0.10g, 0.20g, 0.40g and 0.60g were selected and all input acceleration time histories were PGA-scaled to each of these target PGA_{ref} levels. Further discussion on the suites of time histories used in the pilot study is provided later in this paper.

SSRA Results

All SSRA were conducted using both EL and NL methods, but only the NL results were used to derive $F(T,PGA_{ref})$ functions due to their applicability over a wider range of γ_{cyc} than EL results. The maximum γ during the earthquake, γ_{max}, is highest within the softest layers (between 6 m and 7 m depth where V_s = 148 m/s). For PGA_{ref} up to about 0.2g, the highest γ_{max} in the profile was generally less than about 0.4%, so EL analysis would be adequate to model the NL amplification response. But at PGA_{ref} = 0.4g and 0.6g, the highest γ_{max} in the profile tended to be above 0.3%, with means of 0.9% and 2.4%, respectively, so NL analyses are preferred for modeling the response of this site to such high-intensity ground motions. To maintain consistency at all intensity levels, the EL results were not used in this study.

At each of the 5 intensity levels selected to scale the input time histories, a suite of eleven (11) $F(T,PGA_{ref})_i$ functions for each of the three TRTs were calculated from the ratio of the $S_a(T,PGA_{ref})_{out}$ at ground surface, as calculated from the NL SSRA, to the $S_a(T,PGA_{ref})_{in}$ of each input time history. Linear SSRA were also conducted on the time histories scaled to PGA_{ref} = 0.05g in order to determine the amplification response associated with the linear-elastic properties of the soil at very small strains. The TRT-specific arithmetic mean of each suite of eleven $F(T,PGA_{ref})_i$, $\bar{F}(T,PGA_{ref})$, as determined from linear SSRA and from NL SSRA at each of the five intensity levels, are compared on Figures 2a to 2f. At each intensity level, it is apparent that the TRT-specific mean $\bar{F}(T,PGA_{ref})$ are very similar at T = 0.01 s and at T ≥ 0.05 s. There are more significant differences in the high frequency response from T = 0.02 s to 0.05 s, but this is not a relevant period range for building design.

The main peak in the $\bar{F}(T)$ generated from the linear SSRA (in Figure 2a) occurs between 0.21s and 0.22 s, which is the fundamental period (T_f) of the soil column above the strong impedance contrast at the bedrock interface, based on the linear-elastic dynamic properties of the soil. The linear T_f is consistent with the $T_0 = 4H/(\bar{V}_s)_{soil}$ = 0.22 s computed using the ESL approach. The NL SSRA show a similar peaked amplification response, but T_f increases and $\bar{F}(T_f)$ decreases as the ground motion intensity increases, which causes an increase in γ_{cyc} and a resulting decrease in G and increase in damping. The variation in T_f and $\bar{F}(T_f)$ with PGA_{ref}, which were obtained from the mean of $\bar{F}(T,PGA_{ref})$ from all TRTs, are listed in Table 1. $\bar{F}(T_f)$ from NL SSRA can be seen to decrease with increasing $\ln(PGA_{ref})$ and the logarithmic trend indicates that the linear $\bar{F}(T_f)$ = 4.7 corresponds to PGA_{ref} ≤ 0.02g.

Table 1. Variation in Fundamental Period (T_f) and Amplification at T_f with Ground Motion Intensity.

SSRA Type	PGA_{ref} (g)	Fundamental Period, T_f (s)	Mean $F(T_f)$
Linear	≤0.02	0.22	4.7
Non-Linear	0.05	0.25	3.8
Non-Linear	0.10	0.27	3.2
Non-Linear	0.20	0.32	2.6
Non-Linear	0.40	0.39	2.0
Non-Linear	0.60	0.50	1.8

At $T < T_0$, $\bar{F}(T)$ decreases with increasing PGA_{ref} due to the increase in non-linear hysteretic damping. This behaviour is consistent with the trend of decreasing $F(T,PGA_{ref})$ with increasing PGA_{ref} for Site Classes D and E in NBC 2015. However, the shift of the resonant amplification peak to a longer T_f as the soil column softens with increasing ground motion intensity causes a transition to a trend of increasing $\bar{F}(T,PGA_{ref})$ with increasing PGA_{ref} at $T > T_f(PGA_{ref})$. Such behaviour was not considered by NBC 2015 or the GMMs in SHMC-6 since those GMMs do not account for site period at any ground motion intensity. For "impedance" sites that exhibit peaked amplification behaviour at T_f, the intensity-dependence of T_f presents challenges for development of generic closed-form solutions for intensity-dependent amplification functions that are specific to code-specified periods.

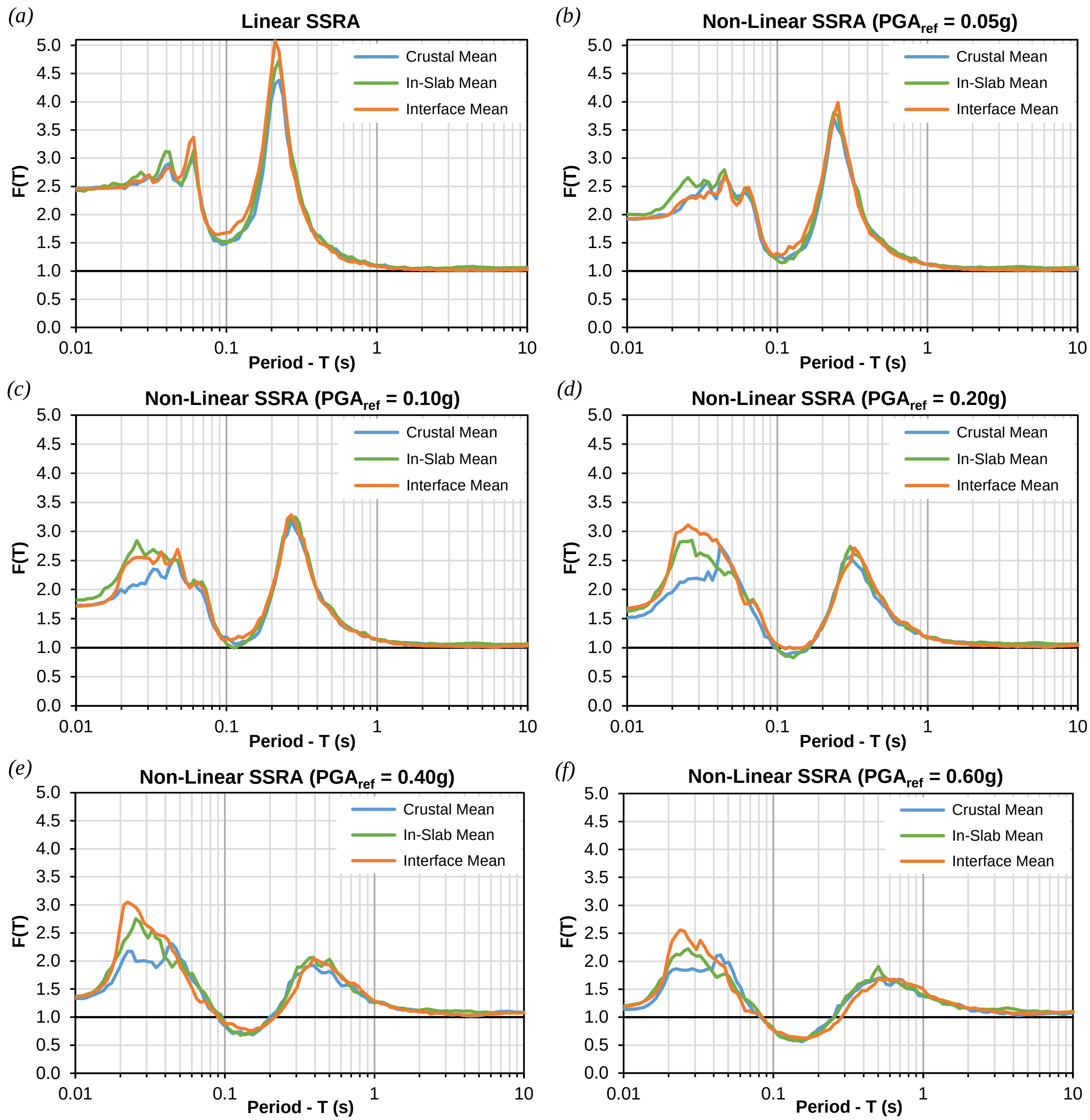

Figure 2. Mean Amplification Functions, $\bar{F}(T,PGA_{ref})$, by Tectonic Regime Type from (a) Linear SSRA, and (b) to (f) Non-Linear SSRA for PGA_{ref} = 0.05g to 0.60g

Implementation in SHMC-6 (Rigorous Method)

Lookup tables of SSRA-derived $\bar{F}(T,PGA_{ref})$ for the three TRTs were generated from the mean amplification functions shown in Figures 2a to 2f. Each table contained mean amplification factors (relative to ground surface values for V_{s30} = 1100 m/s) for PGA_{ref} = 0.01g (from linear SSRA) and for each of the PGA_{ref} considered in the non-linear SSRA (as listed in Table 1), at the following periods (in seconds): 0.01, 0.05, 0.10, 0.15, 0.20, 0.25, 0.30, 0.40, 0.50, 0.60, 0.75, 1.0, 1.5, 2.0, 3.0 and 5.0.

Each of the TRT-relevant GMMs in SHMC-6 was modified to replace its linear and non-linear site terms with the $F(T,PGA_{ref})$ from the TRT-specific lookup table, as described in the companion paper by Bebamzadeh et al., 2023 [2]. For this pilot study, linear interpolation was used to calculate $\bar{F}(T,PGA_{ref})$ for values of the GMM-estimated median PGA_{ref} between the values included in the lookup tables, rather than using period-specific relations between $F(T,PGA_{ref})$ and PGA_{ref}.

The site-specific amplified $S_a(T)$ calculated for each event scenario using the $\bar{F}(T,PGA_{ref})$-modified GMM was combined with the GMM's sigma model for the V_{s30} = 1100 m/s reference condition for calculation of the probabilistic hazard curves [2], which were used to construct SSRA-based UHS for 2%, 5% and 10% probabilities of exceedance in 50 years. The SHMC-6-consistent UHS that were generated from this rigorous implementation of SSRA-derived $F(T,PGA_{ref})$ within SHMC-6 were used as the baseline for comparison to UHS generated using the simplified methods described below.

SIMPLIFIED METHODS OF CALCULATING UHS FROM SSRA

The results of deterministic SSRA can be used to generate the site-specific UHS at a specified annual exceedance rate corresponding to the total aggregated hazard (AER_T), $S_a(T,AER_T)_{SSRA}$, by multiplying the UHS for the reference ground condition, $S_a(T,AER_T)_{ref}$, by a SSRA-generated amplification function, $F(T)_{SSRA}$, that is conditioned on a ground motion intensity measure corresponding to some hazard value associated with the reference ground condition, x_{ref}:

$$S_a(T, AER_T)_{SSRA} = F(T, x_{ref})_{SSRA} \times S_a(T, AER_T)_{ref} \tag{1}$$

Various simplified methods are described by Stewart et al., 2014 [4]. The two methods that are considered in this paper are: i) the UHS Target approach (similar to the "hybrid" method in [4]), and ii) the Median Intensity Target approach (similar to the "modified hybrid" method in [4]).

In the UHS Target method, x_{ref} in Eq. 1 corresponds to an aggregated probabilistic hazard value at the cumulative AER_T. This is consistent with the method used to calculate amplified hazard values in NBC 2015. In that method, PGA_{ref} corresponding to design hazard levels (eg. 2%, 5% or 10% probability of exceedance in 50 years) was used to determine F(T). It has been common practice in Canada to use the UHS as a target spectrum and to spectrally match suite(s) of time histories such that the $S_a(T)$ of each time history closely matches the design UHS over a range of periods that are considered appropriate to each TRT. This method significantly reduces the inter-event variability in the frequency content of the input ground motions and in the SSRA-derived amplified Sa(T). But the acceleration time histories that are input into the SSRA have little to no relevance to the response spectra of individual earthquakes since the shape of the UHS is not representative of individual earthquake response spectra. And since the intensity of the input motions tends to be much higher than the expected intensity of most of the individual event scenarios that contribute to the cumulative AER_T, the UHS-matched time histories will cause the SSRA to overestimate the soil shear strains that would be expected from most or all individual earthquake events, resulting in an overestimation of hysteretic damping and prediction of unrealistic amplification behaviour, particularly for softer soils.

In the Median Intensity Target approach, x_{ref} in Eq. 1 corresponds to the median of the GMM-predicted hazard values (excluding σ) associated with all the individual event scenarios considered by the hazard model (corresponding to individual magnitude-distance scenarios for each TRT) for the specified reference ground condition, denoted as med_x_{ref}. Stewart et al., 2014 [4] compared the results of various simplified methods, including the "hybrid" and "modified hybrid" methods, to the rigorous implementation of non-linear site amplification functions determined from SSRA within the probabilistic seismic hazard analysis (PSHA) for three California sites (Los Angeles, San Francisco and Sacramento). They concluded that the "modified hybrid" approach (similar to the Median Intensity Target approach described in this paper) provided the best comparison to the fully probabilistic implementation.

Median Intensity Hazard Values from Total Hazard Deaggregation Data

In the Median Intensity Target (MIT) approach, "median" refers to the 50th percentile prediction of the hazard value in linear space. The GMM predictions of seismic hazard values for individual event scenarios, x_i, are treated as log-normal distributions that can be described by the mean of $\ln(x_i)$, denoted as μ_x, and the standard deviation in natural logarithm units, σ_x. The log-normal distribution of x_i is equivalent to a normal distribution of $\ln(x_i)$ where the mean and median values of $\ln(x_i)$ are the same, i.e. $med\_ln(x) = \mu_x$. Therefore, when considering log-normally distributed values in linear space, $med\_x = e^{\mu}$.

The aggregated probabilistic hazard value at a specified cumulative AER_T, $x(AER_T)$, can be related to the GMM-predicted x_i via the parameter "epsilon" (ε_x), where ε_x is the number of logarithmic standard deviations (σ_x) between $x(AER_T)$ and x_i. The contribution-weighted mean ε_x from all event scenarios, $\bar{\varepsilon}_x$, is used to relate $x(AER_T)$ to μ_x, as follows:

$$\ln\big(x(AER_T)\big) = \mu_x + \bar{\varepsilon}_x(AER_T) \cdot \overline{\sigma}_x \tag{2}$$

where $\bar{\varepsilon}_x(AER_T)$ increases as AER_T decreases. By substituting $\mu_x = \ln(med\_x)$ in Eq. 2 and re-arranging, the following relation is obtained, which can be used to determine med_x from $x(AER_T)$ if ε_x and σ_x are known:

$$med\_x = \exp\left[\, \ln\big(x(AER_T)\big) - \bar{\varepsilon}_x(AER_T) \cdot \overline{\sigma}_x \,\right] \tag{3}$$

$\bar{\varepsilon}_x$ can be obtained from deaggregation data generated by the OpenQuake engine used to run SHMC-6. An example of the PGA deaggregation data for the V_{s30} = 1100 m/s reference condition at 2% in 50 years PoE (AER_T = 0.000404), for a site in downtown Victoria that is located about 1 km north of the example site used in this study, is presented on Figure 3 (provided by NRCan [5]). The 3D plot indicates the % contribution (on the vertical axis) to the 2%/50-years PGA_{ref} = 0.58g from each "bin" representing a range of event scenario magnitudes (in M0.1 increments) and rupture distances (R in 20 km increments). The columns are also colour-coded to show the relative contributions of different ε_{PGA} bins to the % contribution from each M-R bin to the total probabilistic hazard. Similarly, the % contributions of different ε_{PGA} bins to the aggregated total hazard for PGA(0.000404) are shown above the colour-coded epsilon scale in the upper right corner of Figure 3.

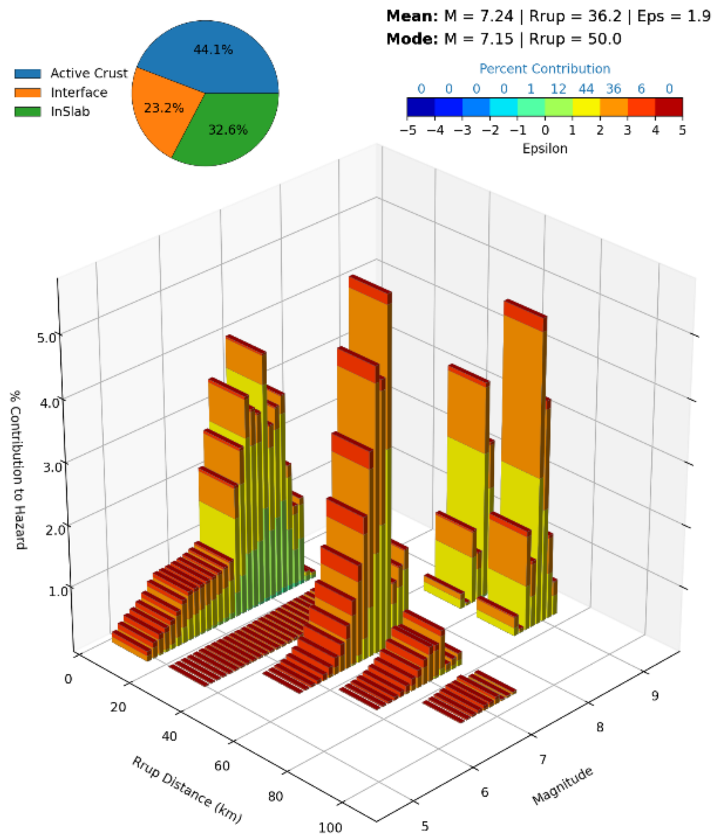

Figure 3. Deaggregation of 2%/50-years PGA_{ref} (V_{s30} = 1100 m/s) for Victoria, BC [5]

To establish a median target spectrum for time history selection purposes, it would be necessary to determine the $\bar{\varepsilon}_x$ from deaggregation of each of the $S_a(T)$ hazard values at the design hazard level. For sites in southwestern BC where there are three TRTs to consider, three sets of TRT-specific $\bar{\varepsilon}_x$ are required to construct the TRT-specific median target spectra. The three sets of TRT-specific $\bar{\varepsilon}_x(0.000404)$ at the example site in Victoria are provided in Table 2 ($\bar{\varepsilon}_{Sa(0.05s)}$ values are not included since deaggregation data for $S_a(0.05s)$ were not obtained). The TRT-weighted mean $\bar{\varepsilon}_{PGA}$ value (according to the TRT contributions from PGA deaggregation, as shown in Figure 3), which is required to determine the *med_PGA*$_{ref}$ associated with the total hazard for the 2%/50-years hazard level, is also included in Table 2.

Table 2. Mean Epsilon for V_{s30} = 1100 m/s reference condition at 2%/50-years Hazard Level by Tectonic Regime

Tectonic Regime	**PGA**	**Response Spectrum Period – T (s)**							
		0.1	**0.2**	**0.3**	**0.5**	**1.0**	**2.0**	**5.0**	**10**
Crustal	1.51	1.57	1.56	1.60	1.61	1.63	1.80	1.54	1.51
In-Slab	2.29	2.33	2.29	2.27	2.19	2.12	2.09	2.12	2.18
Interface	1.96	2.01	1.93	1.83	1.77	1.71	1.60	1.60	1.58
Total Hazard	1.87								

Values of σ_x from each of the eight GMMs for in-slab and interface events, as adopted by SHMC-6 for locations in western Canada, are included in GMM tables included within the Geological Survey of Canada Open File 8630 (Kolaj et al., 2020 [6]), whereas the σ_x models of the active crust GMMs (Abrahamson et al., 2014 [7], Boore et al., 2014 [8], Campbell & Bozorgnia, 2014 [9] and Chiou & Youngs, 2014 [10]) are built into OpenQuake. The mean of the four GMM-specific σ_x values for the in-slab and interface TRTs are provided in Table 3.

The active crust σ_x values are a function of M for linear site response, as well as various parameters to describe non-linear site response when V_{s30} is below the period-dependent threshold values for purely linear response as defined by the various GMMs. The V_{s30} = 1100 m/s reference condition used in this pilot study is at or above the non-linear limits, so only the M dependency needed to be accounted for in this case. The mean of σ_x(M) from all four active crust GMMs, $\overline{\sigma}_x$(M), for each hazard value (x) are plotted on Figure 4. All four active crust GMMs use σ_x that are generally higher for low-M events than for higher M events (eg. Gregor et al., 2014 [11]). It can be seen from Figure 4 that the relation between $\overline{\sigma}_x$(M) and M is generally non-linear, particularly for short-period hazard values. Accordingly, the contribution-weighted mean $\overline{\sigma}_x$ values for the crustal hazard, which are included in Table 3, were calculated by applying each $\overline{\sigma}_x$(M) function to every individual event scenario within the total hazard deaggregation data file for the corresponding hazard value, allowing $\overline{\sigma}_x$(M) to be weighted by the contribution of each event scenario to the crustal hazard integral. Alternatively, the contribution-weighted mean M of the crustal events, $\overline{M}_{cr}$, can be used to calculate $\overline{\sigma}_x(\overline{M}_{cr})$, although the short-period sigma values calculated this way were slightly (about 1% to 2%) lower than the values calculated using the individual event scenarios.

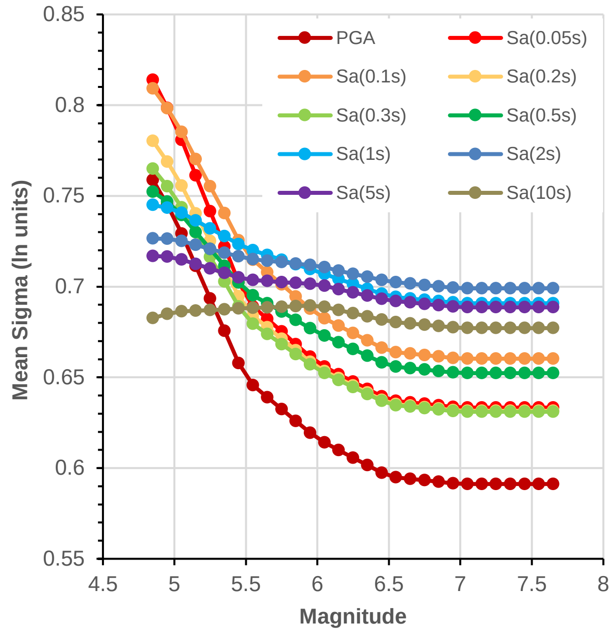

Figure 4. Variation in Mean of Active Crust Sigma Values with Magnitude for Vs30 = 1100 m/s

Table 3. Mean of GMM Sigma Values (ln units) by Tectonic Regime

Tectonic Regime	PGA	Response Spectrum Period – T (s)								
		0.05	**0.1**	**0.2**	**0.3**	**0.5**	**1.0**	**2.0**	**5.0**	**10**
Active Crust*	0.605	0.652	0.676	0.642	0.638	0.657	0.693	0.700	0.690	0.678
In-Slab	0.676	0.712	0.742	0.698	0.688	0.677	0.691	0.693	0.677	0.677
Interface	0.692	0.731	0.768	0.746	0.733	0.704	0.694	0.726	0.701	0.713
Total Hazard	0.642									

*Note: Active Crust $\overline{\sigma}_x$ are specific to V_{s30} = 1100 m/s reference condition and site-specific variation in M

Using the $\bar{\varepsilon}_x$(0.000404) values in Table 2 and the $\overline{\sigma}_x$ values in Table 3 within Eq. 3, the med_x_{ref} target values for the 2%/50-years design hazard level can be determined from the 2%/50-years UHS hazard values obtained from the NBC 2020 Seismic Hazard Tool published online by Natural Resources Canada (NRCan). The site-specific UHS and the med_x_{ref} hazard values for each TRT are provided in Table 4. These define the target response spectra that would be used for selection of the three suits of TRT-specific time histories in accordance with the Median Intensity Target approach. Similarly, med_PGA_{ref} = 0.17g representing the total hazard (all TRTs) is determined from Eq. 3 using the TRT-weighted mean $\bar{\varepsilon}_{PGA}$ = 1.87 from Table 2 and the TRT-weighted mean $\overline{\sigma}_{PGA}$ = 0.642 from Table 3.

Table 4. Site-Specific UHS and Median Hazard Values (g) for V_{s30} = 1100 m/s Reference Condition at 2%/50-years

Target Type	PGA	5% Damped Response Spectrum Accelerations - S_a(T) (T in s)								
		0.05	**0.1**	**0.2**	**0.3**	**0.5**	**1.0**	**2.0**	**5.0**	**10**
Total Hazard UHS	0.579	0.952	1.430	1.320	1.110	0.803	0.444	0.275	0.075	0.033
Crustal Median	0.233	0.35	0.495	0.485	0.400	0.278	0.144	0.078	0.026	0.012
In-Slab Median	0.124	0.18	0.255	0.266	0.234	0.182	0.102	0.065	0.018	0.0075
Interface Median	0.149	0.22	0.305	0.313	0.291	0.232	0.135	0.086	0.024	0.011
Total Hazard Median	0.172									

Input Time History Scaling Approach

In the proposed MIT approach, the median intensity of PGA for the V_{s30} = 1100 m/s reference condition adopted for the SSRA was selected as the IM for determining F(T,x_{ref}) as a function of x_{ref} = med_PGA_{ref}. This is consistent with the approach used by most of the GMMs in SHMC-6. Use of PGA_{ref} as the IM also maintains compatibility between the MIT method and the implementation of F(T,PGA_{ref}) in the Rigorous Method.

The same three suites of 11 input time histories that were used to determine the F(T,PGA_{ref}) implemented in the Rigorous Method were used for conducting SSRA in accordance with the proposed Median Intensity Target (MIT) approach. Each acceleration time history was amplitude-scaled so that $PGA_i = med\_PGA_{ref}$ (0.235g, 0.125g and 0.15g for crustal, in-slab and interface suites, respectively) while maintaining the frequency content of each time history, which results in variability in $S_a(T)_i$ that is a function of the response spectrum attributes of the time histories selected. This is the same scaling approach that was used for the Rigorous Method which involved scaling multiple sets of time histories to different PGA_{ref}. Maintaining consistency between PGA_i and med_PGA_{ref} was considered important to properly predict the peak in $\bar{F}$(T) corresponding to the resonant amplification response of the high impedance example site used in the pilot study, given the dependence of T_f and F(T_f) on PGA_{ref} discussed previously (refer to Table 1). However, this approach is only considered appropriate for deterministic SSRA, not fully probabilistic SSRA which would need to consider all sources of variability in the analysis including variability in PGA_{ref}.

The $S_a(T)_i$ of each suite of med_PGA_{ref} -scaled input time histories are plotted on the semi-log plots in Figures 5a to 5c. On each plot, the geometric mean of the suite of 11 time histories is compared to the target spectrum generated from the $med\_S_a(T)_{ref}$ values in Table 4. There is reasonably good agreement between the geomean of each suite and the target spectrum at T around T_f = 0.3 s, which is the fundamental period of the site at the med_PGA_{ref} intensity levels used in the MIT method. The geomean S_a(0.3s) for the crustal and in-slab suites are 5% and 7% below their respective target S_a(0.3s) values whereas the geomean S_a(0.3s) of the interface suite is 9% above its target S_a(0.3s) value.

Ranges of linear S_a(T) values corresponding to $\ln(med\_S_a(T)_{ref}) \pm \bar{\sigma}_x$ from the SHMC-6 GMMs are also plotted on Figures 5a to 5c. If $\ln(x_{ref})$ predicted by the GMMs is normally distributed, then 68% of the time histories in each suite should ideally have $S_a(T)_i$ that falls between the red dashed lines, or 7 to 8 out of the 11 earthquake records. That means that at any period, it would be reasonable for the $S_a(T)_i$ from one or two earthquake records to plot above and below the dashed lines.

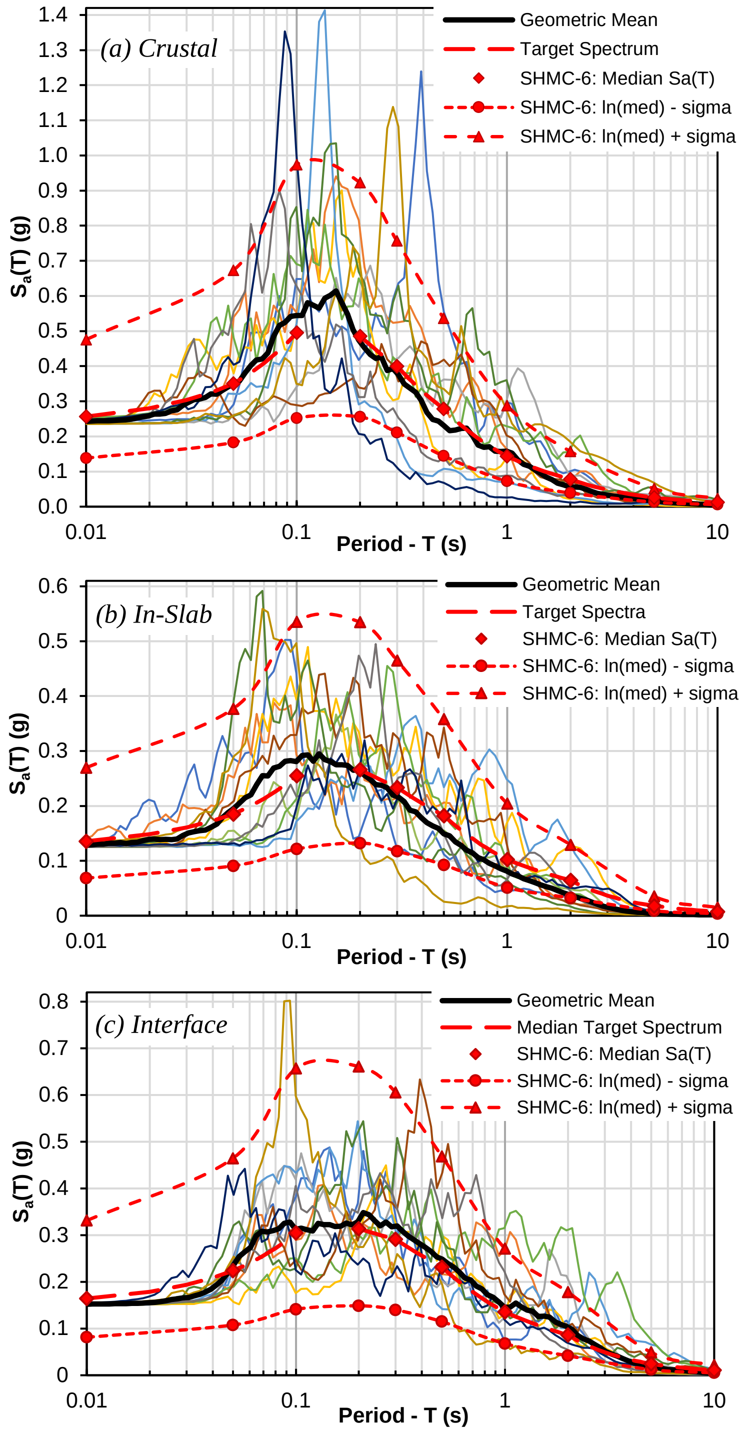

Figure 5. 5% Damped Response Spectra of Input Time Histories: (a) Crustal, (b) In-Slab, (c) Interface

Amplification Functions from Median Intensity Target Method

Consistent with the approach used to determine the F(T,PGA_{ref}) in the Rigorous Method, TRT-specific suites of eleven F(T,med_PGA_{ref})$_i$ functions were calculated from the ratio of output to input response spectra for each earthquake record, which are plotted in Figures 6a to 6c. To maintain consistency with the Rigorous Method, only the F(T,med_PGA_{ref})$_i$ determined from NL SSRA are plotted here. The TRT-specific arithmetic mean of each suite of amplification functions, $\bar{F}$(T,med_PGA_{ref})$_{TRT}$, are also plotted on these figures and compared directly on Figure 6d. The TRT contribution-weighted mean F(T) for the total hazard, $\bar{F}(\mathrm{T})_{\mathrm{TH}}$, which was calculated from Eq. 4 below, is also plotted on Figure 6d.

$$\bar{F}(\mathrm{T})_{TH} = c_{Cr}\bar{F}(T)_{Cr} + c_{InS}\bar{F}(T)_{InS} + c_{Int}\bar{F}(T)_{Int} \quad (4)$$

The TRT contributions in Eq. 4, c_{Cr} = 44.1%, c_{InS} = 32.7% and c_{Int} = 23.2%, are obtained from the total hazard deaggregation of $\mathrm{PGA_{ref}}$ since med_PGA_{ref} is used as the IM in the proposed MIT method.

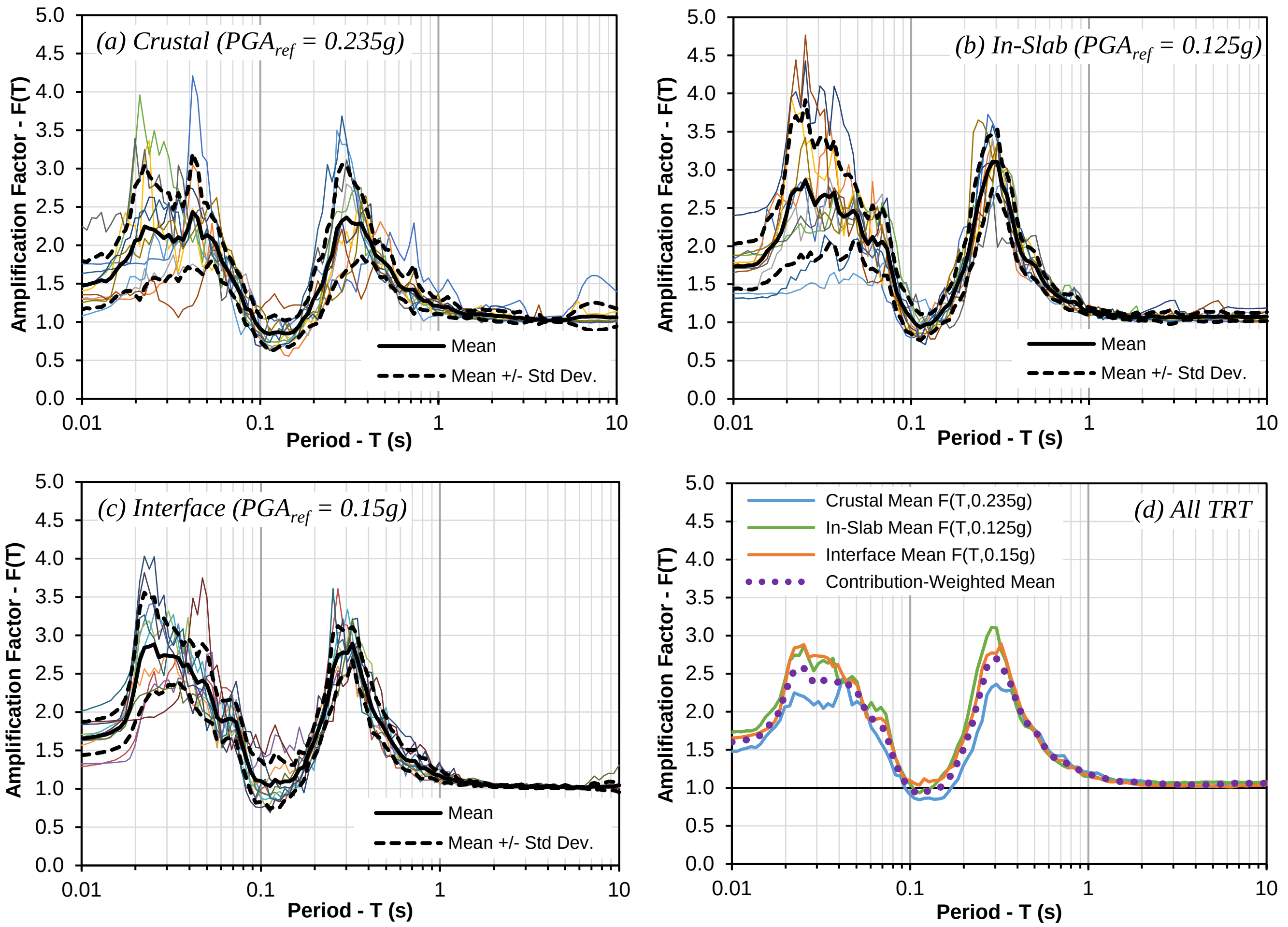

Figure 6. Amplification Functions Conditioned on TRT-Specific PGA_{ref} for (a) Crustal, (b) In-Slab, (c) Interface Suites; (d) TRT-Specific Mean $F(T,PGA_{ref})$ and Contribution-Weighted Mean F(T) for Total Hazard

AMPLIFICATION FUNCTIONS FROM SIMPLIFIED METHODS COMPARED TO RIGOROUS METHOD

On Figure 7, the $\bar{F}(\mathrm{T})_{\mathrm{TH}}$ determined using the proposed MIT method based on 2%/50-years total hazard deaggregation data is compared to the response spectrum ratio (RSR) determined from the ratio of the site-specific 2%/50-years UHS generated using the Rigorous Method to the 2%/50-years $\mathrm{UHS_{ref}}$ corresponding to the V_{s30} = 1100 m/s reference ground condition. In general, very good agreement between these two methods can be observed, which validates the effectiveness of the proposed MIT method. Since the MIT method is based on a single intensity level, the MIT method generates a $\bar{F}_{\mathrm{peak}}$ at $\mathrm{T_f}(med\_PGA_{ref}) \approx 0.3$ s that is slightly higher (+5%) and a $\bar{F}$(0.2s) that is slightly lower (-11%) than the RSR(T) determined from the Rigorous Method which considers the full range of event-scenario med_PGA_{ref}. At all other periods, the $\bar{F}(\mathrm{T})_{\mathrm{TH}}$ determined using the MIT method is almost identical to the RSR(T) from the Rigorous Method.

The contribution-weighted mean of $\bar{F}(\mathrm{T},0.58\mathrm{g})_{\mathrm{TRT}}$, where 0.58g is the 2%/50-years $\mathrm{PGA_{ref}}$ for the site, is also plotted on Figure 7. This is a site-specific example of an amplification function that would be generated using the UHS Target method, which is similar to the current practice of scaling/matching input time histories to the UHS at the design hazard level. When comparing $\bar{F}(\mathrm{T},0.58\mathrm{g})_{\mathrm{TH}}$ to the average amplification calculated within SHMC-6 as demonstrated by the RSR(T) from the Rigorous Method, it can be clearly seen that scaling of time histories to the design UHS produces an amplification function that overpredicts the average T_f and underpredicts $\bar{F}_{peak}$ due to the high intensity of the input ground motions. For the example site analyzed in this study, the UHS Target method underpredicts short-period amplification at T < 0.5 s (by up to 50% at T_f = 0.3 s) and overpredicts long-period amplification at T > 0.5 s (by up to 18% at T = 1 s).

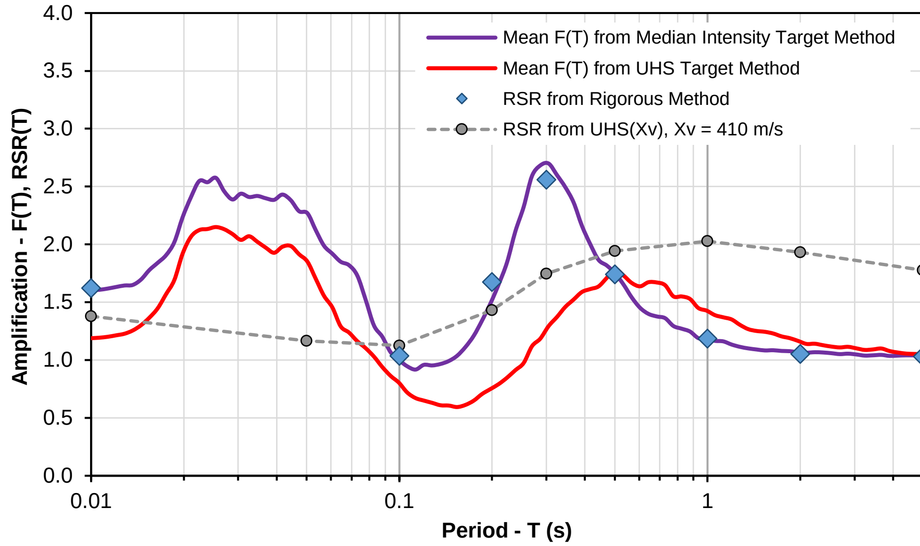

Figure 7. Comparison of Mean Amplification Functions from Median Intensity Target Method and UHS Target Method to Response Spectra Ratio (RSR) from Rigorous Method and from X_v Approach for 2%/50-years Hazard Level

A set of $S_a(T,X_v)$ at 2%/50-years probability of exceedance was obtained from the NRCan Seismic Hazard Calculator for a site designation X_v = 410 m/s corresponding to the site-specific V_{s30} = 407 m/s for the mixed soft soil and bedrock at the example site. The V_{s30}-based RSR(T) corresponding to the ratio of $S_a(T, X_{410})$ to $S_a(T, X_{1100})$ is also plotted on Figure 7 for comparison to the SSRA-based RSR(T) generated using the Rigorous Method. It is apparent from Figure 7 that the average amplification implied by the V_{s30}-based site terms in the GMMs does not properly capture the peaked amplification at T_f = 0.3 s that results from the high impedance contrast located at 9 m depth at the example site. The V_{s30}-based X_v approach significantly underpredicts $\bar{F}_{peak}$ around T_f = 0.3 s and significantly overpredicts amplification at T > 0.5 s. This highlights the importance of using SSRA to identify resonant amplification behaviour of high impedance contrast sites which is not properly captured by the V_{s30}-based GMMs adopted for SHMC-6.

CONCLUSIONS

This paper proposes a deterministic method of calculating the site-specific probabilistic $S_a(T)$ at a design hazard level (the Uniform Hazard Spectrum) by multiplying the probabilistic $S_a(T)$ for the reference ground condition, $S_a(T)_{ref}$, by a mean amplification function, $\bar{F}(T)$, determined from SSRA conducted on input time histories that are scaled to the median PGA of the reference ground condition, *med_PGA*$_{ref}$. This is referred to as the Median Intensity Target (MIT) method. Deaggregation of the probabilistic PGA_{ref} and $S_a(T)_{ref}$ hazard values (generically denoted as *x*) is used to calculate $\bar{\varepsilon}_x$ for each tectonic regime type (TRT), which is a measure of the number of logarithmic standard deviations, σ_x, between ln(*med_x*) and the natural logarithm of the probabilistic hazard value at the specified probability of exceedance. Each GMM adopted by SHMC-6 has its own σ_x model. TRT-specific mean σ_x values, $\bar{\sigma}_x$, are provided in Table 3, but the active crust $\bar{\sigma}_x$ values are specific to the V_{s30} = 1100 m/s reference condition used in this study and the site-specific distribution of crustal magnitudes indicated by the deaggregation data. Using the $\bar{\varepsilon}_x$ values in Table 2 and the $\bar{\sigma}_x$ values in Table 3 within Eq. 3, the *med_x*$_{ref}$ target values for a design hazard level can be determined from the UHS hazard values at that design level as obtained from the NBC 2020 Seismic Hazard Tool. TRT-specific $\bar{F}(T,med\_PGA_{ref})_{TRT}$ are determined from SSRA conducted on each suite of *med_PGA*$_{ref}$-scaled time histories, and the TRT contribution-weighted mean $\bar{F}(T)_{TH}$ for the total hazard is determined from Eq. 4 using the TRT contributions determined from deaggregation of PGA_{ref}.

The results of the MIT method was validated by comparison to the UHS generated using the Rigorous Method which involved replacing the V_{s30}-based site terms within the SHMC-6 GMMs with tables of $\bar{F}(T,PGA_{ref})_{TRT}$ determined from SSRA conducted on the same suite of time histories scaled to multiple PGA_{ref} intensity levels. The modified GMMs then calculate the amplified hazard values for each individual event scenario by applying the SSRA-derived $\bar{F}(T,PGA_{ref})_{TRT}$ to the GMM-estimated median PGA_{ref} for each event scenario. The modified SHMC-6 then probabilistically aggregates the amplified hazard values from all event scenarios to generate a set of total hazard curves that are used to construct the site-specific 2%/50-years UHS.

For the high impedance contrast site considered in this pilot study, the $\bar{F}(T)_{TH}$ determined using the proposed MIT method (with TRT-specific med_PGA_{ref} values derived from deaggregation of the 2%/50-years PGA_{ref}) is shown to be in close agreement with the average amplification function represented by the response spectra ratio, $RSR_{2\%/50yrs}$, determined using the Rigorous Method. In this case, $RSR_{2\%/50yrs}$ is the ratio of the site-specific 2%/50-years UHS to the 2%/50-years UHS_{ref} corresponding to the V_{s30} = 1100 m/s reference ground condition. Conversely, the mean amplification function, $\bar{F}(T,0.58g)_{TH}$, calculated using the UHS Target method, where 0.58g is the 2%/50-years PGA_{ref} for the site, is shown to deviate significantly from the $RSR_{2\%/50yrs}$ determined using the Rigorous Method.

It is recommended that the MIT method be considered when conducting SSRA for projects where hazard values generated by SHMC-6 are being implemented. The UHS Target method should not be used to calculate SSRA-based UHS for projects that have adopted SHMC-6 hazard values due to the tendency for this method to significantly overestimate shear strains and hysteretic damping, which may lead to a significant under-estimation of amplification, particularly at periods around the fundamental period of the site.

ACKNOWLEDGMENTS

The authors would like to gratefully thank Engineers & Geoscientists British Columbia and the members of the Technical Review Board Steering Committee for their support of this research that has been carried out with funding from the BC Ministry of Education for development of the Seismic Retrofit Guidelines for BC school buildings. We would also like to thank Michal Kolaj of Natural Resources Canada for his guidance on the mechanics of seismic hazard calculations within SHMC-6, and Tuna Onur of Onur Seemann Consulting for her suggestions on SSRA implementation within SHMC-6.

REFERENCES

[1] Kolaj, M, Allen, T, Mayfield, R, Adams, J, Halchuk, S. (2019). "Ground-motion models for the 6th Generation Seismic Hazard Model of Canada". *12th Canadian Conference on Earthquake Engineering*, Quebec, QC, June 17-20, 2019.

[2] Bebamzadeh, A., Fairhurst, M., Weech, C., Ventura, C. and Olivera, R. (2023): "Comparison of Methods to Incorporate Site Response Analysis Results into Probabilistic Seismic Hazard Analysis". *Canadian-Pacific Conference on Earthquake Engineering (CCEE-PCEE)*, Vancouver, June 25-30, 2023.

[3] Darendeli, M.B. (2001). *Development of a New Family of Normalized Modulus Reduction and Material Damping Curves.* Ph.D. Thesis, University of Texas at Austin, August, 2001. 362 p.

[4] Stewart, J.P., Afshari, K. and Hashash, Y. (2014). *Guidelines for Performing Hazard-Consistent One-Dimensional Ground Response Analysis for Ground Motion Prediction*. Pacific Earthquake Engineering Research Center, Report PEER 2014/16, October, 2014.

[5] Halchuk, S. (2022) : Personal email, May 10, 2022.

[6] Kolaj, M., Halchuk, S., Adams, J. and Allen, T.I. (2020): "Sixth generation seismic hazard model of Canada: input files to produce values proposed for the 2020 National Building Code of Canada", Geological Survey of Canada Open File 8630, 2020, 15 p.

[7] Abrahamson, N.A., Silva, W.J. and Kamai, R. (2014): "Summary of the ASK14 ground motion relation for active crustal regions", *Earthquake Spectra*, Vol. 30, No. 3, pp. 1025–1055.

[8] Boore, D.M., Stewart, J.P., Seyhan, E. and Atkinson, G.M. (2014): "NGA-West 2 equations for predicting PGA, PGV, and 5%-damped PSA for shallow crustal earthquakes", *Earthquake Spectra*, Vol. 30, No. 3, pp. 1057-1085.

[9] Campbell, K.W. and Bozorgnia, Y. (2014): "NGA-West2 ground motion model for the average horizontal components of PGA, PGV, and 5% damped linear acceleration response spectra", *Earthquake Spectra*, Vol. 30, No. 3, pp. 1087-1115.

[10] Chiou, B.S.-J. and Youngs, R.R. (2014): "Update of the Chiou and Youngs NGA model for the average horizontal component of peak ground motion and response spectra", *Earthquake Spectra*, Vol. 30, No. 3, pp. 1117–1153.

[11] Gregor, N., Abrahamson, N.A., Atkinson, G.M., Boore, D.M., Bozorgnia, Y., Campbell, K.W., Chiou, B.S.-J., Idriss, I.M., Kamai, R., Seyhan, E., Silva, W, Stewart, J.P. and Youngs, R. (2014): "Comparison of NGA-West2 GMPEs", *Earthquake Spectra*, Vol. 30, No. 3, pp. 1179–1197.